An improved SWAT vegetation growth module for tropical ecosystem

Alemayehu T.[1,2*], van Griensven A.[1,2] and Bauwens W.[1]

[1]Vrije Universiteit Brussel (VUB), Department of Hydrology and Hydraulic Engineering, Brussel, Belgium
[2]IHE Delft Institute for Water Education, Department of Water Science and Engineering, Delft, the Netherlands

*Correspondence: t.abitew@un-ihe.org; Tel.: +31-621381512

Abstract. The Soil and Water Assessment Tool (SWAT) is a globally applied river basin eco-hydrological model in a wide spectrum of studies, ranging from land use change and climate change impacts studies to research for the development of best water management practices. However, SWAT has limitations in simulating the seasonal growth cycles for trees and perennial vegetation in the tropics, where rainfall (via soil moisture) is the major plant growth controlling factor than temperature. Our goal is to improve the vegetation growth module of the SWAT model for simulating the vegetation variables such as the leaf area index (LAI) for tropical ecosystem. Therefore, we present a modified SWAT version for the tropics (SWAT-T) that uses a straightforward but robust soil moisture index (SMI) - a quotient of the rainfall (P) and reference evapotranspiration (PET) - to initiate a new growth cycle dynamically within a pre-defined period. Our results for the Mara Basin (Kenya/Tanzania) show that the SWAT-T simulated LAI corresponds well with the Moderate Resolution Imaging Spectroradiometer (MODIS) LAI for evergreen forest, savanna grassland and shrubland, indicating that the SMI is reliable for triggering new growth cycle annually. The water balance components (evapotranspiration and streamflow) simulated by the SWAT-T exhibit a good agreement with a thermal-based evapotranspiration (ET-RS) estimate and observed streamflow. The SWAT-T model with the proposed improved vegetation growth module for tropical ecosystem can be a robust tool for simulating the vegetation growth dynamics consistently in hydrologic model applications including land use and climate change impact studies.

1. Introduction

The Soil and Water Assessment Tool (SWAT; Arnold et al., 1998) is a process-oriented, spatially semi-distributed and time-continuous river basin model. SWAT is one of the most widely applied eco-hydrological models for simulating hydrological and biophysical processes under a range of climate and management conditions (Arnold et al., 2012; Bressiani et al., 2015; Gassman et al., 2014; van Griensven et al., 2012; Krysanova and White, 2015). Many studies used SWAT in tropical Africa, to investigate the basin hydrology (e.g. Dessu and Melesse, 2012; Easton et al., 2010; Mwangi et al., 2016; Setegn et al., 2009) as well as to study the hydrological impacts of land use change (e.g. Gebremicael et al., 2013; Githui et al., 2009; Mango et al., 2011) and climate change (Mango et al., 2011; Mengistu and Sorteberg, 2012; Setegn et al., 2011; Teklesadik et al., 2017). Notwithstanding the high number of SWAT model applications in tropical catchments, only a few studies underscored the limitation of its plant growth module for simulating the growth cycles of trees, perennials and annuals in this region of the world (Mwangi et al., 2016; Strauch and Volk, 2013; Wagner et al., 2011).

It is worthwhile to note that phenological changes in vegetation affect the biophysical and hydrological processes in the basin hydrology and thus play a key role in integrated hydrologic and ecosystem modeling (Jolly and Running, 2004; Shen et al., 2013; Strauch and Volk, 2013; Yang and Zhang, 2016; Yu et al., 2016). The Leaf Area Index (LAI), a vegetation attribute commonly used in eco-hydrological modeling, strongly correlates with a vegetation phenological development. Thus, an enhanced representation of the LAI dynamics can improve the predictive capability of hydrologic models, as noted in several studies (Andersen et al., 2002; Yu et al., 2016; Zhang et al., 2009). Arnold *et al*. (2012) also underscored the need for a realistic representation of the local and regional plant growth processes to simulate reliably the water balance, the erosion, and the nutrient yields using SWAT. For instance, the LAI and canopy height are needed to determine the canopy resistance and the aerodynamic resistance to subsequently compute the potential plant transpiration in SWAT. Therefore, inconsistencies in the vegetation growth could result in uncertain ET estimates as noted in Alemayehu *et al.* (2015).

SWAT utilizes a simplified version of the Environmental Policy Impact Climate (EPIC) crop growth module to simulate the phenological development of plants, based on accumulated heat units (Arnold et al., 1998; Neitsch et al., 2011). SWAT uses dormancy, which is a function of daylength and latitude, to repeat the annual growth cycle for trees and perennials. Admittedly, this approach is suitable for temperate region. However, Strauch and Volk (2013) showed that the LAI temporal dynamics are not well represented for perennial vegetation (savanna and shrubs) and evergreen forest in Brazil. Likewise, Wagner et al. (2011) reported a mismatch between the growth cycle of deciduous forest in the Western Ghats (India) and the SWAT dormancy period, and they subsequently shifted the dormancy period to the dry season.

Unlike temperate regions where the vegetation growth dynamics are mainly controlled by the temperature, the primary controlling factor in tropical regions is the rainfall (i.e. the water availability) (Jolly and Running, 2004; Lotsch, 2003; Pfeifer et al., 2012, 2014; Zhang, 2005). A study of Zhang et al. (2005) explored the relationship between the rainfall seasonality and the vegetation phenology across Africa. They showed that the onset of the vegetation green-up can be predicted using the cumulative rainfall as a criterion to indicate the season change. Jolly and Running (2004) determined the timing of leaf flush in an ecosystem process simulator (BIOME-BGC) after a defined dry season in the Kalahari, using events where the daily rainfall (P) exceeded the reference evapotranspiration (PET). They showed that the modeled leaf flush dates compared well with the leaf flush dates estimated from the Normalized Difference Vegetation Index (NDVI), indicating the reliability of a proxy derived from P and PET to pinpoint a season change of tropical ecosystems. Sacks et al. (2010) studied the relationships between crop planting dates and temperature, P and PET globally, using 30-year average climatological values. They noted that in rainfall limited regions the ratio of P to PET is a better proxy for the soil moisture status than is P alone. Using soil moisture index (SMI) derived from the ratio of P to PET to trigger new growth cycle annually in hydrological modeling is appealing because as the SMI can be determined *a priori*. On the other hand, Strauch and Volk (2013) used

SWAT model simulated soil moisture in the top soil layers with a certain minimum threshold after a defined dry season to indicate the start of a rainy season (SOS) and thus new vegetation growth cycle. Their results showed improvements in the SWAT simulated LAI seasonal dynamics and reproduced well the Moderate Resolution Imaging Spectroradiometer (MODIS) 8-day LAI. However, such approach requires calibrating the SWAT parameters for a realistic representation of the soil water balance dynamics often using observed streamflow. Recently, Yu *et al.* (2016) concluded uncertainty in soil moisture is significantly greater than streamflow simulations of a calibrated hydrologic model.

The objective this study is to improve the vegetation growth module of SWAT model for trees and perennials in the tropics. Towards this the use of the SMI within a predefined transition months as a dynamic trigger for new vegetation growth cycle will be explored. The modified SWAT (SWAT-T) model will be evaluated using 8-day MODIS LAI and thermal-based ET. Additionally, the model will be evaluated using observed daily streamflow.

2. Materials and methods

2.1. The study area

The Mara River, a transboundary river shared by Kenya and Tanzania, drains an area of 13,750 km^2 (Figure 1a). This river originates from the forested Mau Escarpment (about 3000 m.a.s.l.) and meander through diverse agroecosystems and subsequently crosses the Masai-Mara Game Reserve in Kenya and the Seregenti National Park in Tanzania and finally feeds the Lake Victoria. The Amala River and the Nyangores River are the only perennial tributaries draining the head water region. The Talek River and the Sand River are the two most notable seasonal rivers stemming from Loita Hills.

Rainfall varies spatially mainly due to its equatorial location and its topography. The rainfall pattern in most part of the basin is bimodal, with a short rainy season (October-December) driven by convergence and southward migration of the Intertropical Convergence Zone (ITCZ) and a long rainy season (March-May) driven by southeasterly trades. In general, rainfall decreases from west to east across the basin while temperature increases southwards. The Mara basin is endowed with significant biodiversity features through a sequence of zones from moist montane forest on the escarpment through dry upland forest to scattered woodland and then the extensive savanna grasslands (Figure 1b). Dark volcanic origin soils are common on the escarpment and rangelands while shallow soils that drain freely are found lower down. Poorly drained soils cover the plateau and the plains.

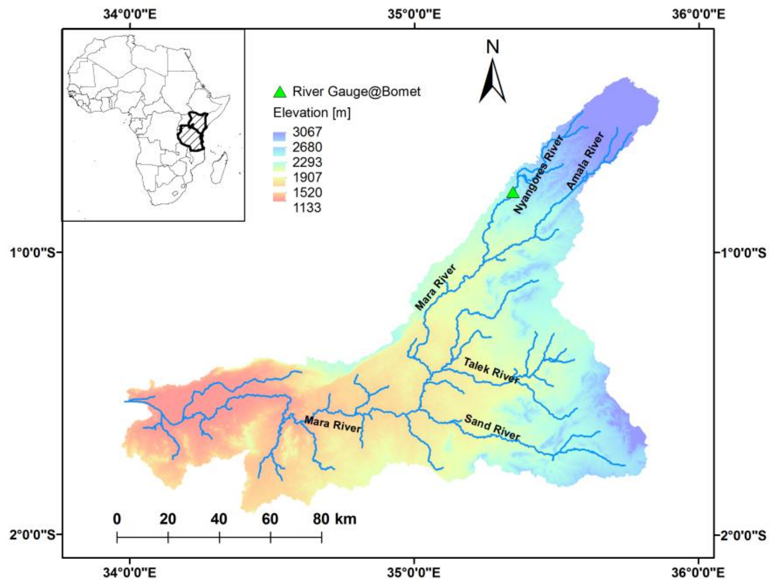

(a)

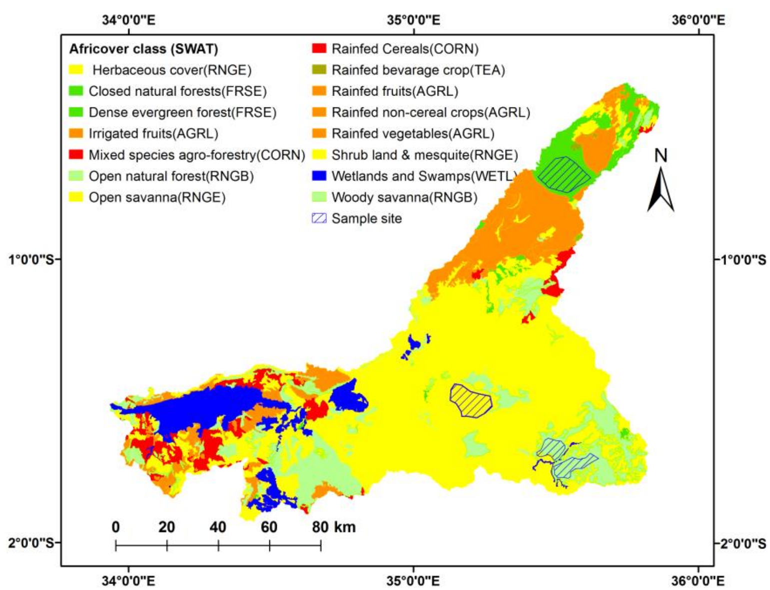

(b)

Figure 1 Location of the Mara Basin (a) and its land cover classes (b). Note the sample sites location for the major natural vegetation classes that are used to mask the Moderate Resolution Imaging Spectroradiometer (MODIS) Leaf Area Index (LAI).

2.2. SWAT model description

The SWAT (Arnold et al., 1998, 2012; Neitsch et al., 2011) is a comprehensive, process-oriented and physically-based eco-hydrological model at a river basin scale. SWAT requires specific information about weather, soil properties, topography, vegetation, and land management practices occurring in the watershed to directly model physical processes associated with water movement, sediment movement, crop growth, nutrient cycling, etc. In SWAT a basin is partitioned into several sub-basins using topographic information and the sub-basins, in turn, are subdivided into several Hydrological Response Units (HRUs) with a unique combination of land use, soil and slope class. Each hydrologic processes are simulated at HRU level on a daily or sub-daily time step and aggregated into sub-basin level for routing into a river network (Neitsch et al., 2011). SWAT considers five storages: snow, canopy storage, the soil profile with up to ten layers, a shallow aquifer and a deep aquifer to calculate the water balance (Neitsch et al., 2011) using the following equation:

$$\Delta S = \sum_{i=1}^{t} \left(P - Q_{total} - ET - Losses \right) \tag{1}$$

where ΔS is the change in water storage (mm) and t is time in days. P, $Q_{total,}$ ET and *Losses* are the daily amounts of precipitation (mm), the total water yield (mm), the evapotranspiration (mm) and the groundwater losses (mm), respectively. The total water yield represents an aggregated sum of the surface runoff, the lateral flow and the return flow. In this study, the surface runoff is computed using the Soil Conservation Service (SCS) Curve Number (CN) method (USDA SCS, 1972).

SWAT provides three options for estimating PET: Hargreaves (Hargreaves et al., 1985), Priestley-Taylor (Priestley and Taylor, 1972), and Penman-Monteith (Monteith, 1965) (Neitsch et al., 2011). The model simulates evaporation from soil and plants separately as described in Ritchie (1972). The potential soil evaporation is simulated as a function of PET and leaf area index (LAI) and further reduced with high plant water use while the actual soil water evaporation is estimated by using exponential functions of soil depth and water content (Neitsch et al., 2011). SWAT simulated LAI is also required to calculate the potential plant transpiration with formulations that varies depending on the PET method selection (Alemayehu et al., 2015; Neitsch et al., 2011). The actual plant transpiration (i.e. the plant water uptake) is reduced exponentially for soil water below filed capacity. Therefore, actual evapotranspiration in SWAT refers to the sum of evaporation from the canopy, the soil as well as plant transpiration.

In this study, we use the Penman-Monteith method (Monteith, 1965) to compute the PET for alfalfa (Neitsch et al., 2011) as:

$$PET = \frac{\Delta.\left(H_{net} - G\right) + \rho_{air}.c_p.\left[e_z^o - e_z\right]/r_a}{\Delta + \gamma.\left(1 + {r_c}/{r_a}\right)} \tag{2}$$

where PET is the maximum transpiration rate (mm d^{-1}), Δ is the slope of the saturation vapour pressure-temperature curve (kPa $^{\circ}C^{-1}$), H_{net} is the net radiation (MJ m^{-2} d^{-1}), G is the heat flux density to the ground (MJ m^{-2} d^{-1}), ρ_{air} is the air density (kg m^{-3}), C_p is the specific heat at constant pressure (MJ kg^{-1} $^{\circ}C^{-1}$), e_z^0 is the saturation vapour pressure of air at height z (kPa), e_z is the water vapor pressure of air at height z (kPa), γ is the psychrometric constant (kPa °C^{-1}), r_c is the plant canopy resistance (s m^{-1}), and r_a is the diffusion resistance of the air layer (aerodynamic resistance) (s m^{-1}). The plant growth module simulates LAI and canopy height, which are required to determine the canopy and aerodynamic resistance.

2.3. The vegetation growth and Leaf Area Index modeling in SWAT

SWAT simulates the annual vegetation growth based on the simplified version of the EPIC plant growth model (Neitsch et al., 2011). The potential plant phenological development is hereby simulated on the basis of daily accumulated heat units under optimal conditions; however, the actual growth is constrained by temperature, water, nitrogen or phosphorous stress (Arnold et al., 2012; Neitsch et al., 2011).

Plant growth is primarily based on temperature and hence each plant has its own temperature requirements (i.e. minimum, maximum and optimum). The fundamental assumption in the heat unit theory is plants have a heat unit requirements that can be quantified and linked to the time of planting and maturity (Neitsch et al., 2011). The total number of heat units required for a plant to reach maturity must be provided by the user. The plant growth modeling includes simulation of the leaf area development, light interception and conversion of intercepted light into biomass assuming a plant species-specific radiation-use efficiency (Neitsch et al., 2011). The optimal leaf area development during the initial period of the growth is modeled (Neitsch et al., 2011) as:

$$fr_{LA\mathrm{Im}x} = \frac{fr_{PHU}}{fr_{PHU} + \exp(l_1 - l_2 . fr_{PHU})} \tag{3}$$

where fr_{LAImx} is the fraction of the plant's maximum leaf area index corresponding to a given fraction of potential heat units for the plant, , and l_1 and l_2 are shape coefficients. Once the maximum leaf area index is reached, LAI will remain constant until the leaf senescence begins to exceed the leaf growth. Afterwards, the leaf senescence becomes the dominant growth process and hence the LAI follows a linear decline (Neitsch et al., 2011). However, Strauch and Volk (2013) showed the advantage of using a logistic decline curve, to avoid that the LAI drops to zero before dormancy occurs. Therefore, we adopted this change to SWAT2012 whereby the LAI during leaf senescence for trees and perennials is calculated as (Strauch and Volk, 2013):

$$LAI = \frac{LAI_{mx} - LAI_{\min}}{1 + \exp(-t)} \tag{4}$$

$$with \;\; t = 12(r - 0.5) \quad and \quad r = \frac{1 - fr_{PHU}}{1 - fr_{PHU,sen}} \quad , fr_{PHU} \geq fr_{PHU,sen}$$

where the term used as exponent is a function of time and t varies from 6 to -6, *LAI* is the leaf area for a given day and declines using r as a decline rate, LAI_{mx} and LAI_{min} are the maximum and minimum (i.e. during dormancy) leaf area index, respectively, $fr_{PHU,sen}$ is the fraction of growing season (PHU) at which senescence becomes the dominant growth process.

As detailed in Neitsch *et al.* (2011), the daily LAI calculation for perennials and trees are slightly different, for the latter the years of development is considered.

For perennials, the leaf on day *i* is calculated as:

$$\Delta LAI_i = \left(fr_{LA\mathrm{Im}\,x,i} - fr_{LA\mathrm{Im}\,x,i-1}\right).LAI_{mx}.\left(1-\exp\left(5.(LAI_{i-1}-LAI_{mx})\right)\right) \tag{5}$$

The total leaf area index, the area of green leaf per unit area of land, is calculated:

$$LAI_i = LAI_{i-1} + \Delta LAI_i \tag{6}$$

where ΔLAI_i is the leaf area added on day *i*, LAI_i and LAI_{i-l} are the leaf area indices for day *i* and *i-1* respectively, $fr_{LAImx,i}$ and $fr_{LAImx,i-1}$ are the fraction of the plant's maximum leaf area index for day *i* and *i-1*, LAI_{mx} is the maximum leaf area index for the plants, yr_{cur} is the age of the tree (years), and $yr_{fulldev}$ is the number of years for tree species to reach full development (years).

2.4. SWAT annual vegetation growth cycle limitation for the tropics

SWAT assumes that trees and perennial vegetation can go dormant as the daylength nears the minimum daylength for the year. Dormancy, which is a function of latitude and daylength during which plants do not grow, is used to repeat the growth cycle each year for trees and perennials. At the beginning of the dormant period, a fraction of the biomass is converted to residue and the leaf area index is set to the minimum value (Neitsch et al., 2011). In the tropics, however, plants growth dormancy is primarily controlled by precipitation (Bobée et al., 2012; Jolly and Running, 2004; Lotsch, 2003; Zhang et al., 2010; Zhang, 2005) and hence the standard SWAT growth module cannot realistically represent the seasonal growth dynamics for trees and perennials. SWAT offers several management settings for the start and the end of growing season based on either heat units (the default) or calendar date scheduling. In fact, the limitation with plant growth dynamics cannot be solved using SWAT management settings as far as the latitude and daylength dependent dormancy is activated.

2.5. A soil moisture index-based vegetation growth cycle for the tropics

As several studies demonstrated (Jolly and Running, 2004; Zhang, 2005; Zhang et al., 2006), the water availability in the soil profile is one of the primary governing factors of vegetation growth in tropics. Thus, we propose a soil moisture index (SMI) to trigger new growth cycle for tropical ecosystem in SWAT model within a predefined period. The SMI is computed as:

$$SMI = \frac{\sum_{i=1}^{N} P}{\sum_{i=1}^{N} PET} \tag{7}$$

where P and PET denotes daily rainfall and potential evapotranspiration (mm d^{-1}), N is the number of days of aggregation. In this study we used five days aggregated P and PET (i.e. pentad) to determine the SMI to assure sufficient soil moisture availability to initiate new growth cycle. The SMI is somewhat similar to the Water Requirement Satisfaction Index (WRSI) (Verdin and Kalver 2002), which is a ratio of ET to PET.

Figure 2 presents the SMI seasonal pattern based on long-term climatological P for several gauge stations and PET from Trabucco and Zomer **(**2009**)** across the Mara Basin. It is apparent from Figure 2 that the dry season (mostly from June - September) shows low SMI values (less than 0.5). Additionally, these patterns resemble well the long-term monthly average LAI for the savanna ecosystem (the dominant cover in the mid-section of the Mara Basin). In areas with a humid climate (i.e. the head water regions of the basin), the SMI values are high and the rainfall regime is different, yet in the relatively drier months (January and February) the SMI is low. As shown in Figure 2, the LAI and the SMI seasonal dynamics match well with approximately one month lag, indicating the reliability of the SMI as a proxy for the SOS and hence to trigger the annual vegetation growth cycle. This approach enables SWAT growth module not only to simulate the vegetation cycle dynamically within a predefined period, also avoids the need for management setting (“plant” and “kill”).

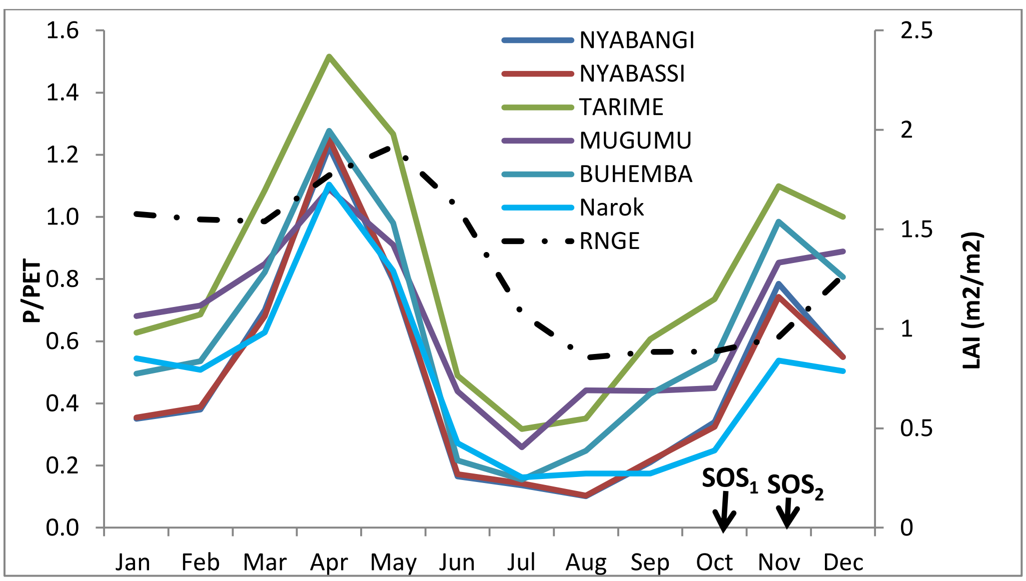

Figure 2 The climatological moisture index (SMI) derived from historical gauge observation across the Mara Basin and Trabucco and Zomer (2009) **global reference evapotranspiration data. Leaf Area Index (LAI) for the savanna ecosystem (dotted line). SOS_1 and SOS_2 represent the start-of-rainy season (SOS) transition months to trigger growth.**

To avoid false starts during the dry season, the end of the dry season and the beginning of the rainy season (SOS_1 and SOS_2, respectively) are determined using a long-term monthly climatological P to PET ratio (Figure 2). For river basins with a single rainfall regime, a single set of SOS months can be used across the basin. However, in basins with different rainfall regimes, different SOS months need to be set at sub-basin level. In our study area two distinct rainfall regimes are observed and therefore two different SOS values were needed. For the major part of the sub-basins October (SOS_1) and November (SOS_2) were used as transitions (Figure 2).

2.6. SWAT-T: the adaptation of the SWAT plant growth module

Based on the rationale elaborated in the preceding sections, we modified the standard SWAT2012 (version 627) plant growth subroutine for basins located between 20^0 N and 20^0 S:

i) If the simulation day is within SOS_1 and SOS_2 for a given HRU and a new growing cycle is not initiated yet, the SMI is calculated as the ratio of the pentad P to PET.

ii) If the SMI exceeds or equals 0.5, a new growing cycle for trees and perennials is initiated. Subsequently, FR_{PHU} is set to 0 and the LAI is set to the minimum value. Plant residue decomposition and nutrient release is calculated as if dormancy would occur.

iii) In case the SMI is still below the threshold (i.e. 0.5) at the end of month SOS_2, a new growing cycle is initiated immediately after the last date of SOS_2.

It is worth noting that SMI threshold could be raised or lowered depending on the climatic condition of the basin.

2.7. Data for model evaluation

The Leaf Area Index

The remote sensing LAI data used in this study is based on the MODIS TERRA sensor (Table 1). The LAI product retrieval algorithm is based on the physics of radiative transfer in vegetation canopies (Myneni et al., 2002) and involves several constants (leaf angle distribution, optical properties of soils and wood, and canopy heterogeneity) (Bobée et al., 2012). The theoretical basis of the MODIS LAI product algorithm and the validation results are detailed in Myneni et al. (2002). Kraus (2008) validated the MOD15A2 LAI data at Budongo Forest (Uganda) and Kakamega Forest (Kenya) sites and reported an accuracy level comparable to the accuracy of field measurements, indicating the reliability of MOD15A2 LAI for evaluating SWAT simulated LAI for the study area.

Table 1 Summary of the inputs of the SWAT model and the evaluation datasets.

	Spatial/temporal resolution	Source	Description
Rainfall	5 km / 1-day	Roy *et al.* (2017)	Bias-corrected satellite rainfall for Mara basin
Climate	25 km / 3-hour	Rondell *et al.* (2004)	Max. and min. temperature, relative
Land cover classes	30 m	FAO (2002)	Land cover classes for East Africa

DEM	30 m	NASA (2014)	Digital elevation model
Soil classes	1 km	FAO (2009)	Global soil classes
Discharge	Daily (2002-2008)	WRMA (Kenya)	River discharge at Bomet
ET	1 km / 8-day	Alemayehu *et al.* (2017)	ET maps for Mara basin
MOD15A2	1 km / 8-day	LPDAAC(2014)	Global leaf area index

We selected a representative relatively homogeneous sample sites (i.e. polygons) for evergreen forest (174 km^2), tea (123 km^2), savanna grassland (136 km^2) and shrubland (130 km^2) (see Figure 1b) using the Africover classes and Google Earth images. This is useful to reduce the effect of land cover mix while averaging coarse scale (i.e. 1 km) LAI and hence improve the reliability of the LAI timeseries. Subsequently, the MOD15A2 LAI was masked using the polygons of the sample covers and pixels with only quality flag 0, which indicates good quality, were used. Also, pixels with LAI values less than 1.5 during the peak growing months (i.e. period with LAI values mostly above 2.0) were removed. Finally, we extracted the 8-day median LAI time series for each land cover for 2002-2009 and few gaps in the LAI time series were filled using linear interpolation. Notwithstanding with all the quality control efforts, due to the high variability and the inevitable signal noise, we noted breaks and high temporal variation in the LAI timeseries (Figure 3). Verbesselt et al. (2010) developed the Breaks For Additive Seasonal and Trend (BFAST) method that decomposes the Normalized Vegetation Index (NDVI) time series into trend, seasonal, and remainder components. The trend and seasonal components comprise information pertinent to phenological developments as well as gradual and abrupt changes whereas the reminder component comprises noise and error information of the time series. This method has been applied to tropical ecosystems to identify phenological cycles as well as abrupt changes (DeVries et al., 2015; Verbesselt et al., 2010, 2012). In our study, we used the BFAST tool to extract the seasonal development pattern of LAI while excluding the noise and error information from the LAI timeseries. Figure 3 demonstrates the smoothed 8-day LAI time series using BFAST along with the raw-median LAI values. It is apparent from the smoothed LAI time series that the high LAI development occurs during the wet months from March to May, suggesting consistency in the smoothed LAI timeseries. Therefore, the smoothed LAI time series were used to calibrate and evaluate the SWAT-T model vegetation growth module for simulating LAI.

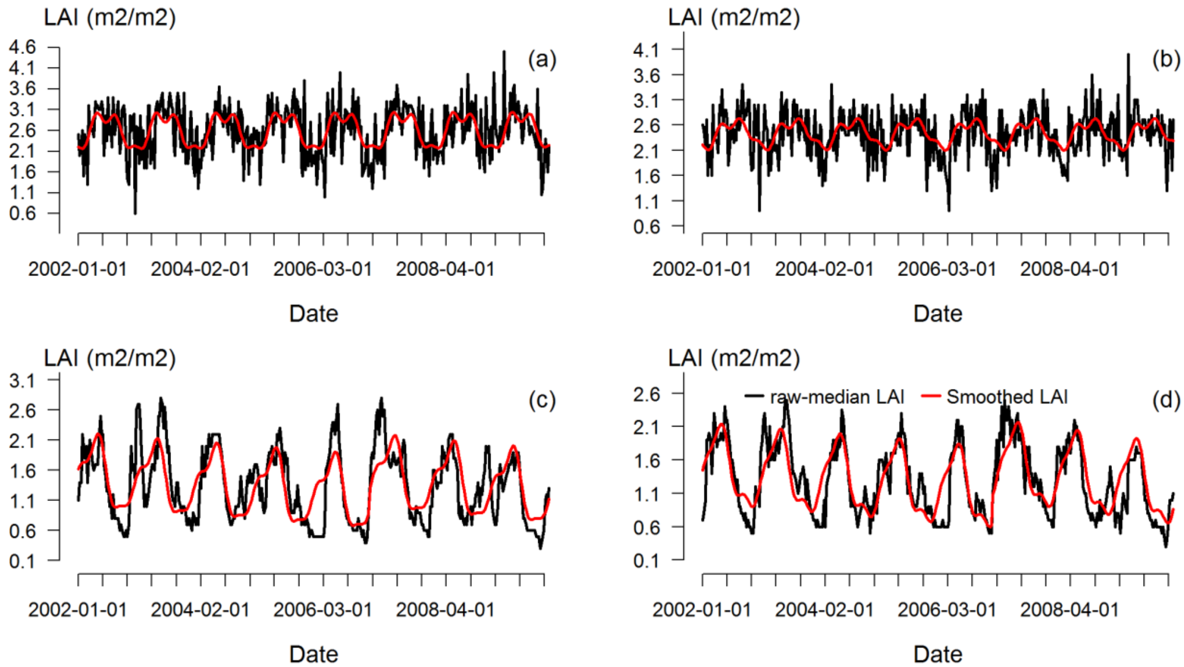

Figure 3 The 8-day raw-median LAI timeseries for evergreen forest (a), tea (b), grassland (c) and shrubland (d) sample sites. The raw-median LAI is smoothed using the Breaks For Additive Seasonal and Trend (BFAST) method (Verbesselt et al., 2010).

The evapotranspiration

ET is one of the major components in a basin water balance that is influenced by the seasonal vegetation growth cycle. Thus, remote sensing-based ET estimates can be used to evaluate (calibrate) the SWAT-T model. Alemayehu et al. (2017) estimated ET for the Mara River basin using several MODIS thermal imageries and the GLDAS global weather dataset from 2002 to 2009 at a 8-day temporal resolution based on the Operational Simplified Surface Energy Balance (SSEBop) algorithm (Senay et al., 2013). The SSEBop mainly depends on the remotely sensed land surface temperature and the grass reference evapotranspiration (Senay et al., 2013). Alemayehu et al. (2017) demonstrated that the SSEBop ET explained about 52%, 63% and 81% of the observed variability in the MODIS NDVI at 16-day, monthly and annual temporal resolution. Also, they suggested that the estimated ET can be used for hydrological model parameterization. We note the resemblance in the seasonal pattern of the MODIS LAI analyzed in this study with the SSEBop ET, hereafter referred as remote sensing-based ET (ET-RS). Therefore, we used this dataset to evaluate the SWAT-T simulated ET at land cover level.

Streamflow

Due to the limited availability of observed streamflow, we used daily observed streamflow series (2002-2008) for the head water region (700 km^2) at Bomet gauging station. The streamflow data is relatively complete with about 11% missing gaps distributed throughout the timeseries.

2.8. Model set up, calibration and evaluation

2.8.1. The model set up and data used

The Mara River Basin was delineated using a high resolution (30 m) digital elevation model (DEM) (NASA, 2014) in ArcSWAT2012 (revision 627). The basin was subdivided into 89 sub-basins to spatially differentiate areas of the basin dominated by different land use and\ or soil with dissimilar impact on hydrology. Each sub-basin was further discretized into several HRUs, which represent unique combinations of soil, land use and slope classes. The model was set up for conditions representing the period 2002-2009. The land cover classes for the basin were obtained from FAO-Africover project (FAO, 2002). Generally speaking, as shown in Figure 1b, the dominant portion of the basin is covered by natural vegetation including savanna grassland, shrubland and evergreen forest. These land cover classes were assigned the characteristics of RNGE, RNGB and FRSE, respectively in SWAT (Neitsch et al., 2011). We extracted the soil classes for the basin from the Harmonized Global Soil Database (FAO, 2008). A soil properties database for the Mara River Basin was established using the soil water characteristics tool (SPAW, http://hydrolab.arsusda.gov/soilwater).

The list of hydro-climatological and spatial data used to derive the SWAT model are presented in Table 1. In situ measurements of rainfall and other climate variables are sparse and thus bias-corrected multi- satellite rainfall analysis data from Roy et al. (2017) were used. The bias-correction involves using historical gauge measurements and a downscaling to a 5 km resolution. Detailed information on the bias-correction and downscaling procedures can be found in Roy *et al.* (2017). Weather data needed to compute the PET using the Penman-Monteith (Monteith, 1965) method was obtained from the Global Land Data Assimilation System (GLDAS) (Rodell et al., 2004). To remove the biases in the PET estimates compared to observation based long-term (1950-2000) seasonal PET (Trabucco and Zomer, 2009) estimates, we slightly adjusted the solar radiation for each month at sub-basin level.

2.8.2. Model calibration and evaluation approach

The main purpose of this study is to explore the potential of the SMI to trigger new vegetation growth cycle for the tropical ecosystem within a predefined period annually. We initially evaluated the effects of the vegetation growth module modification by comparing against the standard SWAT model growth module with varying management settings. This analysis involved uncalibrated simulations of the SWAT models with the default SWAT model parameters, meaning the models differs only with how vegetation growth is simulated. It is worth noting that the aim of these simulations is mainly to expose the inconsistencies in the vegetation growth module structure. Afterwards, we calibrated the parameters related to the simulation of the LAI, the evapotranspiration and the streamflow manually by trial-and-error and expert knowledge for the SWAT-T model. Firstly, SWAT parameters that control the shape, the magnitude and the temporal dynamics of LAI were adjusted to reproduce the MODIS LAI at 8-day for each land cover classes. Then, we adjusted parameters that mainly control streamflow and evapotranspiration (ET) simulation simultaneously using the daily observed streamflow and 8-day ET-RS. Perhaps, the manual adjustment may not be as robust as an automatic calibration as the latter explores a larger parameters space. However, the manual calibration is sufficient to illustrate the impact of the modification on the vegetation growth cycle and its effect on the water balance components. The SWAT-T model calibration and validation was done for 2002-2005 and 2006-2009, respectively.

2.8.3. The model performance metrics

The Pearson correlation coefficient (r) and the Percent of PBIAS (%bias) were used to evaluate the agreement between the simulated and the remote sensing-based estimates of LAI and evapotranspiration for each land cover class and the streamflow. Additionally, the model performance was evaluated using the Kling-Gupta Efficiency (KGE) (Gupta et al., 2009), which provides a compressive assessment by taking into account of the variability, the bias and the correlation in a multi-objective sense.

3. Results and discussion

3.1. Consistency assessment of the vegetation growth module without calibration

3.1.1. LAI simulation

To highlight the added value of the modified vegetation growth module in SWAT-T for simulating the seasonal growth pattern of trees and perennials, we compared the daily simulated LAI of the standard SWAT2012 (revision 627) model and SWAT-T model. At this stage, the models were uncalibrated (i.e. based on default SWAT parameters). This is useful to explore the effect of the vegetation growth module structural modification on the consistency of simulated LAI annual cycle. We note from the simulation results considerable inconsistencies in the growth cycle of the simulated daily LAI mainly due to the vegetation growth model structure and management settings. For instance, Figure 4 and Figure 5 present the simulated daily LAI for FRSE and RNGE based on the standard SWAT model under different management settings and the SWAT-T model. Strauch and Volk (2013), Kilonzo (2014) and Mwang et al. (2016) reported similar observations. The default management setting in the standard SWAT model for starting the new growth cycle (i.e. planting) and ending the growth cycle is scheduled using the FR_{PHU} (Heat unit). Thus, the start and the end of the vegetation growth cycle management settings occurs at FR_{PHU} 0.15 and 1.2, respectively. With this management setting, the simulated LAI is zero at the beginning of each simulation year for all types of vegetation cover. Mwang et al. (2016) improved the SWAT LAI simulation with this management setting using FR_{PHU} of 0.001 to start the growing season and minimum LAI of 3.0 for evergreen forest. Yet, this change is region specific and cannot be transferred. As shown in Figure 4 and Figure 5, this can also be partly improved using a date scheduling (Date) for the start and the end of the vegetation growth cycle (i.e. instead of heat unit). Additionally, all the management setting can be removed (no mgt) and vegetation is growing since the start of the simulation (i.e. IGRO=1).

The forested head-water region experiences a unimodal rainfall regime, with March-August being the rainy season. In contrast, a bimodal rainfall regime prevails (March-May and October-December) on the remaining part of the basin. Despite the changes in the management settings, it is apparent that the standard SWAT model has inherent limitation to simulate vegetation growth cycle for tropics that are consistent with seasonal rainfall distribution (Figure 4 and Figure 5). Also, the vegetation growth cycle resets annually on 28th June due to dormancy.

In contrast, the simulated LAI cycles for FRSE, tea, RNGE and RNGB cover types using the SWAT-T model (i.e. the modified vegetation growth module) reveal a consistent annual cycle and are associated with the seasonal rainfall pattern (see Figure 4 and Figure 5).

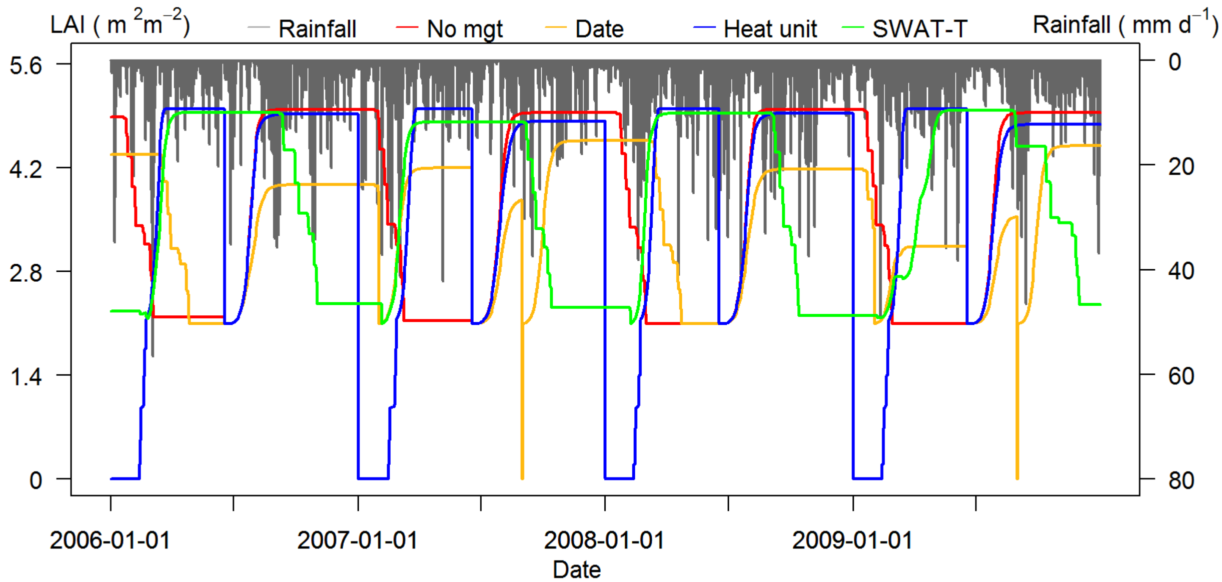

Figure 4 The LAI as simulated by the SWAT-T and the standard SWAT models for different management settings for evergreen forest (FRSE) using default SWAT parameter. See management settings explanations in the texts.

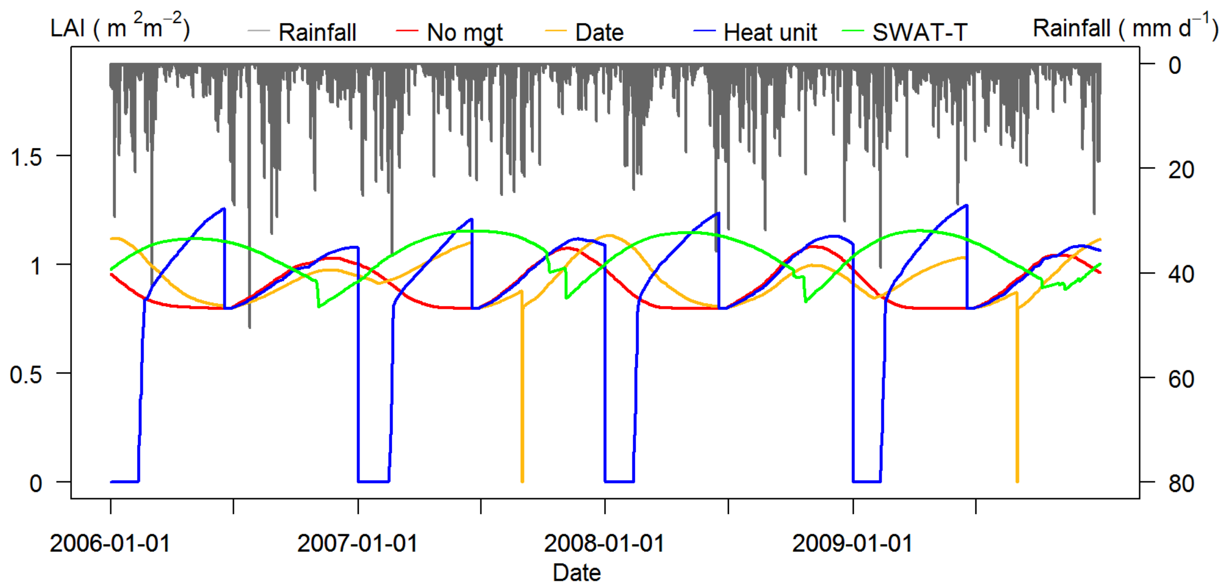

Figure 5 The LAI as simulated by the SWAT-T and the standard SWAT models for different management settings for grassland (RNGE) using default SWAT parameter. See management settings explanations in the texts.

3.1.2. Implication of inconsistent LAI simulation

The LAI is required to compute potential transpiration, potential soil evaporation and plant biomass, among others in SWAT (Neitsch et al., 2011). For instance, to compute the daily potential plant transpiration in SWAT, the canopy resistance and the aerodynamic resistance are determined using the simulated actual daily LAI and canopy height, respectively (Neitsch et al., 2011). Therefore, the aforementioned limitations of the annual vegetation growth cycle in the standard SWAT model growth module also influence directly the accuracy of transpiration. For instance, Figure 6 depicts the comparison of the standard SWAT and the SWAT-T simulated daily potential transpiration timeseries for grassland based on the Penman-Monteith approach. We observe 14% (12%) of the standard SWAT simulated daily potential transpiration timeseries (2002-2009) for FRSE (RNGE) being zero, suggesting a considerable inconsistency. However, the SWAT-T reduced considerably (i.e. less than 2% for FRSE and RNGE) the inconsistent zero daily potential transpiration, indicating the improvements in the vegetation growth module. Several studies have shown the effect of PET method selection in SWAT on simulated ET and other water balance components (Alemayehu et al., 2015; Maranda and Anctil, 2015; Wang et al., 2006). Alemayehu et al. (2015) reported significant differences in both potential and actual transpiration with the choice of PET method using calibrated SWAT model, which partly ascribed to the unrealistic LAI growth cycle. We notice the SWAT-T simulated potential transpiration is consistent regardless of the PET method selection in SWAT (results not shown here) and therefore, the improved vegetation growth module in the SWAT-T could reduce the uncertainty arising from the module structure and thus minimize the uncertainties in model simulation outputs.

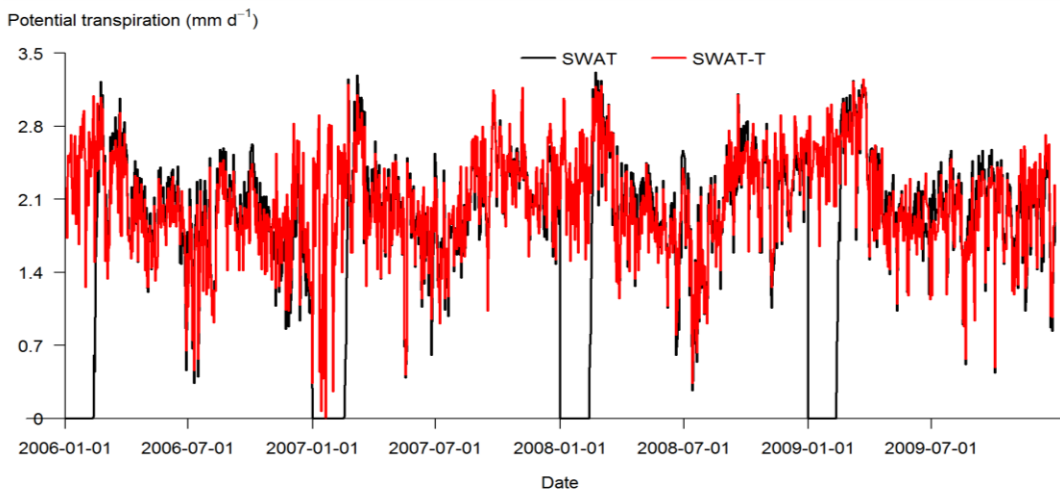

Figure 6 Inter-comparison of Penman-Monteith-based daily potential transpiration simulated by the SWAT-T and the standard SWAT models for grassland. Note that the heat unit scheduling is used in the standard SWAT model.

3.2. Evaluation of the calibrated SWAT-T model

3.2.1. Performance of the LAI simulation

Table 2 presents the list of SWAT model parameters that are adjusted during the calibration process. Initially, the minimum LAI (ALAI_MIN) for each land cover classes were set based on the long-term MODIS LAI. Also, the PHU was computed using the long-term climatology, as suggested in Strauch and Volk (2013). The shape coefficients for the LAI curve ($FRGW_1$, $FRGW_2$, $LAIMX_1$, $LAIMX_2$ and *DLAI*) and the remaining parameters were adjusted during the calibration period by a trail-and-error process such that the SWAT-T simulated 8-day LAI mimics the MODIS 8-day LAI.

Figure 7 presents the comparison of 8-day MODIS LAI with the calibrated SWAT-T simulated LAI aggregated over several land cover classes for the calibration and validation period. We evaluated the degree of agreement qualitatively -by visual comparison- and quantitatively -by statistical measures. From the visual inspection it is apparent that the intra-annual LAI dynamics (and hence the annual growth cycle of each land cover class) from the SWAT-T model correspond well with the MODIS LAI data. This observation is supported by correlation as high as 0.94 (FRSE) and 0.92 (RNGB) during the calibration period (Table 3). As shown in Table 3, the model also shows similar performance during the validation period with low average biases and correlation as high as 0.93 (FRSE). Overall, the results indicate that the SMI can indeed be used to dynamically trigger a new growing season within a predefined period.

Despite the overall good performance of SWAT-T in simulating LAI, we observed biases for FRSE and Tea mainly during the rainy season over the calibration and validation period (see Figure 7 top row). This is partly attributed to the cloud contamination of the MODIS LAI, as shown in Figure 3a and Figure 3b, in the mountainous humid part of the basin , as note in Krause (2008). Also, the senescence seems to occur slightly early for Tea, as shown in Figure

3b, thereby we note a mismatch between SWAT simulated LAI and MODIS LAI. This indicate the need to further adjust the Fraction of total PHU when leaf area begins to decline (DLAI).

Table 2 List of SWAT parameters used to calibrate LAI, ET and streamflow with their default and calibrated values.

			Default (calibrated)		
Parameter	Parameter definition (unit)	Variable	FRSE	RNGE	RNGB
BIO_E	Radiation-use efficiency*((kg/ha)/(MJ/m²))*	LAI	15 (17)	34 (10)	34 (10)
BLAI	Maximum potential leaf area index (m^2/m^2)	LAI	5 (4.0)	2.5 (3.5)	2 (3.5)
$FRGW_1$	Fraction of PHU corresponding to the 1st point on the optimal leaf area development curve	LAI	0.15 (0.06)	0.05 (0.2)	0.05 (0.2)
$LAIMX_1$	Fraction of BLAI corresponding to the 1st point on the optimal leaf area development curve	LAI	0.7 (0.15)	0.1 (0.1)	0.1 (0.1)
$FRGW_2$	Fraction of PHU corresponding to the 2nd point on the optimal leaf area development curve	LAI	0.25 (0.15)	0.25 (0.5)	0.25 (0.5)
$LAIMX_2$	Fraction of BLAI corresponding to the 2nd point on the optimal leaf area development curve	LAI	0.99 (0.30)	0.7 (0.99)	0.7 (0.99)
DLAI	Fraction of total PHU when leaf area begins to decline	LAI	0.99 (0.30)	0.35 (0.99)	0.35 (0.99)
T_OPT	Optimal temperature for plant growth (ºC)	LAI	30 (25)	25 (30)	25 (30)
T_BASE	Minimum temperature for plant growth (ºC)	LAI	0 (5)	12 (5)	12 (5)
ALAI_MIN	Minimum leaf area index for plant during dormant period ($m^2.m^2$)	LAI	0.75 (2.0)	0 (0.75)	0 (0.75)
PHU	Total number of heat units needed to bring plant to maturity	LAI	1800 (3570)	1800 (4100)	1800 (4100)
SOL_Z[1]	Soil layer depths (mm)	ET	300 [1000] (480 [1600])	300[1000] (480 [1600])	300[1000] (480 [1600])
SOL_AWC[2]	Soil available water (mm)	ET/flow	0.26-0.31 [0.27-0.29] (0.18-0.21	0.26-0.31 [0.27-0.29] (0.18-0.21	0.26-0.31 [0.27-0.29] (0.18-0.21

			[0.18-0.20])	[0.18-0.20])	[0.18-0.20])
ESCO	Soil evaporation compensation factor (-)	ET	0.95 (0.88)	0.95 (1)	0.95 (1)
EPCO	Plant uptake compensation factor (-)	ET	1 (1)	1 (1)	1 (1)
GSI	Maximum stomatal conductance at high solar radiation and low vapor pressure deficit ($m.s^{-1}$)	ET	0.002 (0.006)	0.005 (0.0035)	0.005 (0.004)
REVAPMN	Depth of water in the aquifer for revap (mm)	ET	750 (100)	750 (100)	750 (100)
CN2[3]	Initial SCS curve number II value (-)	flow	55 [70] (38 [48])	69 [79] (81 [92])	61 [74] (71 [87])
SURLAG	Surface runoff lag time (day)	flow	4(0.01)	4(0.01)	4(0.01)
ALPHA_BF	Baseflow recession constant (day)	flow	0.048 (0.2)	0.048 (0.2)	0.048 (0.2)
GWQMN	Shallow aquifer minimum level for base flow	flow	1000 (50)	1000 (50)	1000 (50)
GW_REVAP	Groundwater 'revap' coefficient (-)	ET	0.02 (0.1)	0.02 (0.02)	0.02 (0.02)
RCHRG_DP	Deep aquifer percolation fraction (-)	flow	0.05 (0.3)	0.05 (0.1)	0.05 (0.1)

[1]SOL_Z values for the top [and lower] soil layers depth

[2]SOL_AWC values range for the top [and lower] soil layers depending on soil texture and bulk density

[3]CN2 values for soil hydrologic group B[C]

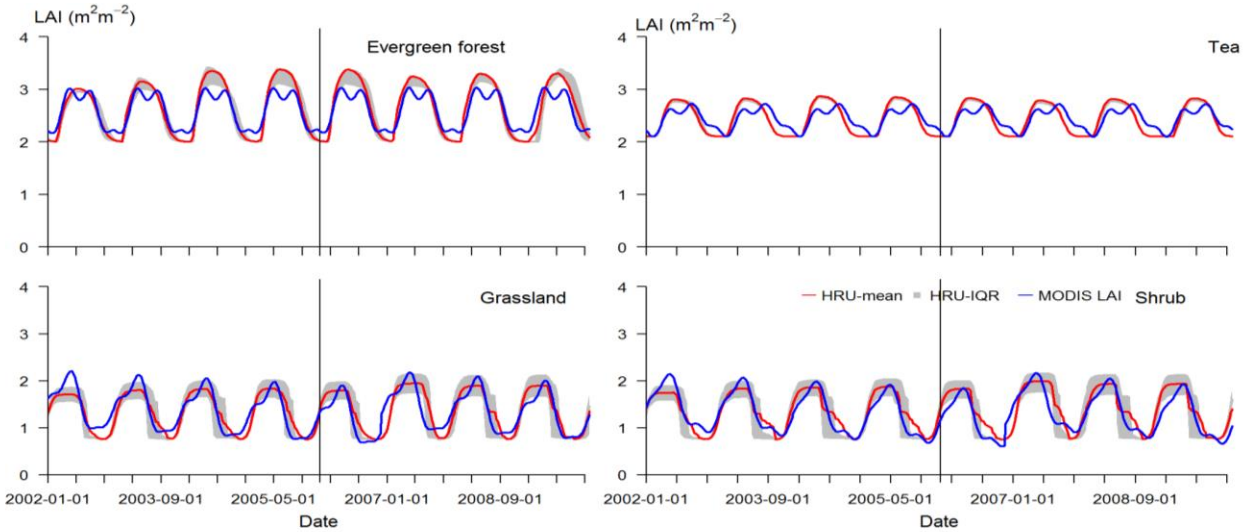

Figure 7 The MODIS LAI and the SWAT-T model simulated HRU weighted aggregated 8-day LAI time series (2002-2009). The gray sheds indicate the boundaries of the 25th and 75th percentiles. The vertical line marks the end of the calibration period and the beginning of the validation period.

Table 3 Summary of the performance metrics for the SWAT-T for simulating LAI, ET and flow. Note that the for LAI and ET the performance is at 8-day whilst daily for flow.

	LAI calibration (validation)				**ET calibration (validation)**				**Streamflow calibration (validation)**
	FRSE	**Tea**	**RNGE**	**RNGB**	**FRSE**	**Tea**	**RNGE**	**RNGB**	**Flow**
r	0.94 (0.93)	0.83 (0.83)	0.89 (0.86)	0.92 (0.88)	0.71 (0.68)	0.67 (0.64)	0.72 (0.77)	0.66 (0.72)	0.72 (0.76)
%bias	1.5 (0)	0.1 (0.2)	-3.7 (-0.4)	-1.3 (4.6)	3.7 (6.6)	-1.7 (0.5)	7.8 (11)	1.2 (2.9)	3.5 (15.5)
KGE	0.50 (0.62)	0.42 (0.44)	0.86 (0.85)	0.88 (0.86)	0.71 (0.67)	0.62 (0.62)	0.69 (0.74)	0.66 (0.72)	0.71 (0.71)

3.2.2. The seasonal vegetation growth pattern

The seasonal pattern of LAI for FRSE, Tea, RNGE and RNGB are analysed using 8-day LAI timeseries (2002-2009) from calibrated SWAT-T model and MODIS LAI. Generally, not surprisingly, the seasonal dynamics of SWAT-T simulated LAI and MODIS LAI agrees well (Figure 8 left) with pooled correlation of 0.97.

As shown in Figure 8 (right), the SWAT-T simulated monthly average LAI shows a higher seasonal variation as compared to the variation observed from MODIS LAI for FRSE with amplitude (i.e. peak-to-trough difference) is about 47.7% and 31%, respectively of the average annual MODIS LAI. The seasonal variation from MODIS LAI is comparable with the results of Myneni *et al*. (2007) who noted 25% seasonal variation in the Amazon forest. We notice a correlation up to 0.66 between the seasonal LAI and rainfall in the humid part of the basin. Our observations are in agreement with Kraus (2008), that reported the association of LAI dynamics for forest sites located in Kenya and Uganda with inter-annual climate variability.

In part of the basin where there is a marked dry season, the seasonal LAI dynamics exhibit a notable seasonal variation, with amplitude (i.e. peak-to-trough difference) that is up to 79% of the mean annual LAI (1.4 m^2/m^2) for RNGE. Unlike the LAI of FRSE and Tea in the humid part, the seasonal rainfall pattern is strongly correlated (up to 0.81) with lagged LAI for RNGE and RNGB. This results is in agreement with several studies that noted that the LAI dynamics for natural ecosystem in the Sub-Saharan Africa are associated with the rainfall distribution pattern (Bobée et al., 2012; Kraus et al., 2009; Pfeifer et al., 2014).

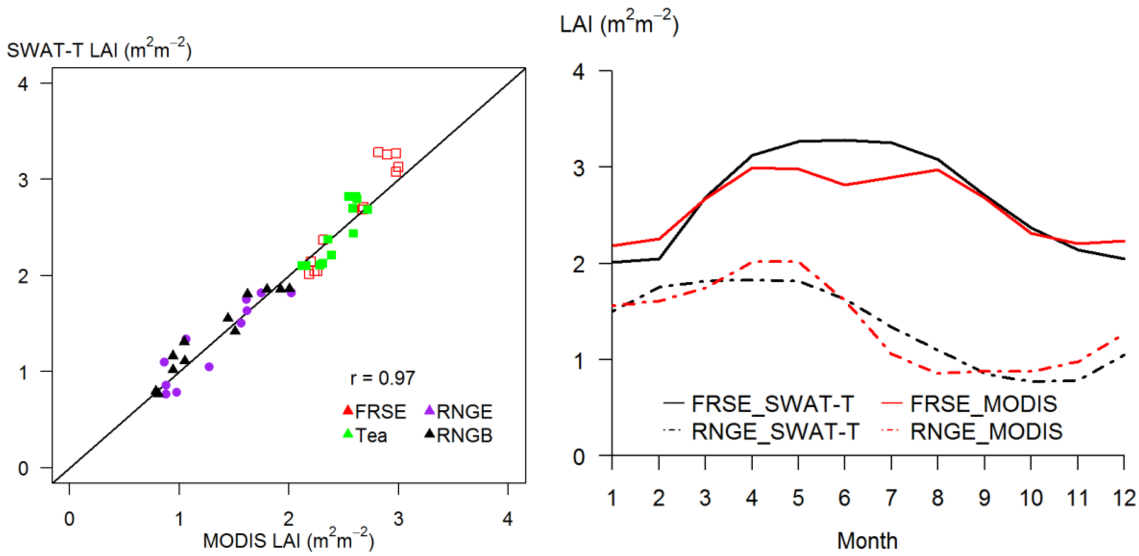

Figure 8 The long-term (2002-2009) average seasonal LAI pooled scatter plot (left) and temporal dynamics (right). FRSE: evergreen forest; RNGE: grassland; RNGB: shrubland.

In addition to improving the seasonal dynamics of LAI in SWAT without the need of management settings, the SMI accounts for the year-to-year shifts in the SOS due to climatic variations. This is particularly important for long-term land use change and climate change impact studies. Figure 9 demonstrates the year-to-year shifts as well as the spatial variation in the SOS dates for part of the Mara River Basin dominated by savanna grassland. Generally, the season change tends to occur in the month of October (i.e. Julian date 278-304). Yet, we acknowledge the need of further verification studies in basins with sufficient forcing data and field measurements.

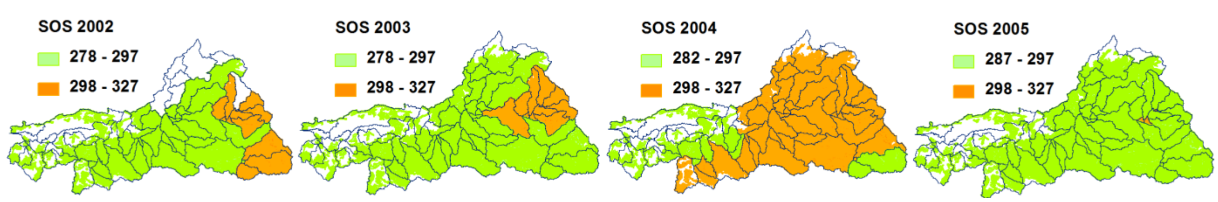

Figure 9 The inter-annual and spatial variation of the start of the rainy season for the savanna vegetation in the Mara River basin for 2002-2005. Note that Julian dates are used and the mapping is done at HRU scale.

3.2.3. The spatial simulation of the evapotranspiration

As presented in Table 2, several SWAT parameters were calibrated by comparing SWAT-T model simulated ET with ET-RS. The higher water use by FRSE as compared to other land cover classes is reflected by a lower ESCO, and a higher GW_REVAP and GSI (Table 2). The lower ESCO indicates an increased possibility of extracting soil water to satisfy the atmospheric demand at a relatively lower soil depth. Also, the higher GW_REVAP points to an increased extraction of water by deep-rooted plants from the shallow aquifer or pumping. Similar findings were reported by Strauch and Volk (2013).

Figure 10 presents the comparison of 8-day ET-RS and SWAT-T simulated ET for the calibration (2002 - 2005) and validation (2006 - 2009) periods for FRSE, Tea, RNGE and RNGB. Visually, the ET simulated by the SWAT-T fairly agrees with the ET-RS for all the covers. As shown in Table 3, the statistical performance indices show a modest performance in simulating ET for the dominant cover types in the basin. The average model biases for the simulated ET ranges from 7.8% (RNGE) to 1.2% (RNGB) during the calibration period. Additionally, the correlation between 8-day ET from the SWAT-T and the ET-RS varies from 0.67 (Tea) to 0.72 (grassland). Overall, we mark similar performance measures during the calibration and validation period, suggesting a fair representation of the processes pertinent to ET.

The variability of the ET is controlled by several -biotic and abiotic- factors. The 8-day ET time series as simulated by the SWAT-T model illustrates the variation in the temporal dynamics of ET in the study area. For land cover types located in the humid part of the basin (FRSE and tea) there is no clear temporal pattern (Figure 10). In contrast, the areas covered by RNGE and RNGB show a clear seasonality in the simulated ET. These observations are consistent with the seasonality of the simulated LAI, as discussed section 3.2.2.

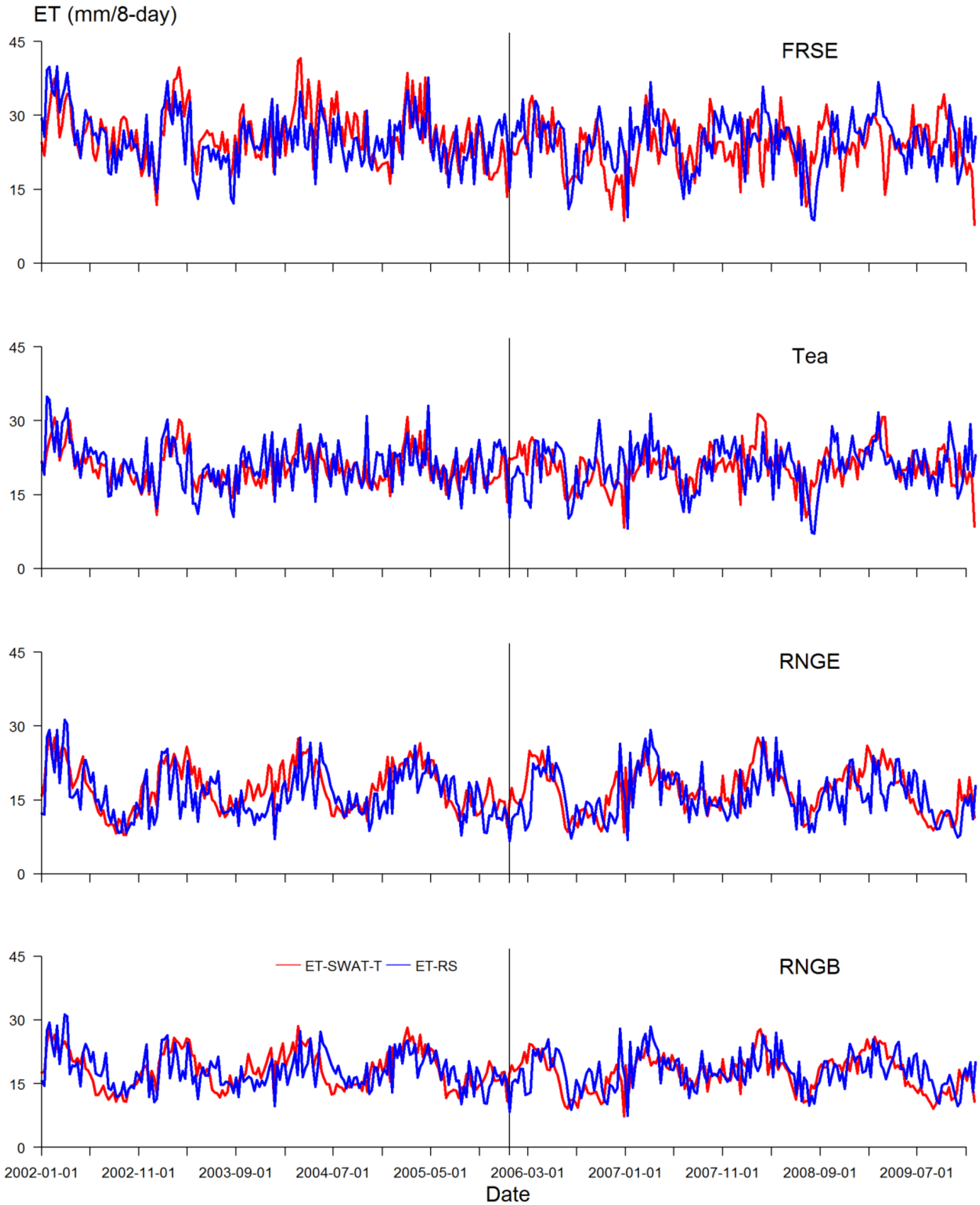

Figure 10 The comparison of remote sensing-based evapotranspiration (ET-RS) and SWAT-T simulated ET (ET-SWAT-T) aggregated per land cover classes. Note that for SWAT-T HRU level ET is aggregated per landcover. The vertical black line marks the end of the calibration period and the beginning of the validation period.

To shed light on the consistency of SWAT-T model simulated LAI and ET, we selected simulation outputs for April and August at HRU level (Figure 11 and Figure 12). Figure 11 (upper row) exhibits the monthly ET at HRU level for the wet month (April) and dry month (August) in 2002. The lower portion of the basin, with dominant savanna cover, experiences a monthly ET between 16 and 63 mm/month in August and between 41 and 93 mm/month in April. These estimates are also well reflected in the spatial distribution of the average monthly simulated LAI (Figure 11 lower row). We notice that the linear relationship between ET and LAI is stronger, in general, for grassland and shrubs than for evergreen forest and tea. The lower correlation for tea and evergreen forest could be partly attributed to the high evaporation contribution of the wet soil, as the upper portion of the basin receives ample rainfall year round. Also, the tea harvesting activities in the upper part of the basin is not taken into account in the model. We also note visually that during the wet month the spatial variability of ET is higher than that of the LAI (Figure 11). Further comparison research is needed to evaluate the added value of the improved vegetation growth module on spatial ET simulations. This will be addressed in our ongoing research on ET evaluation.

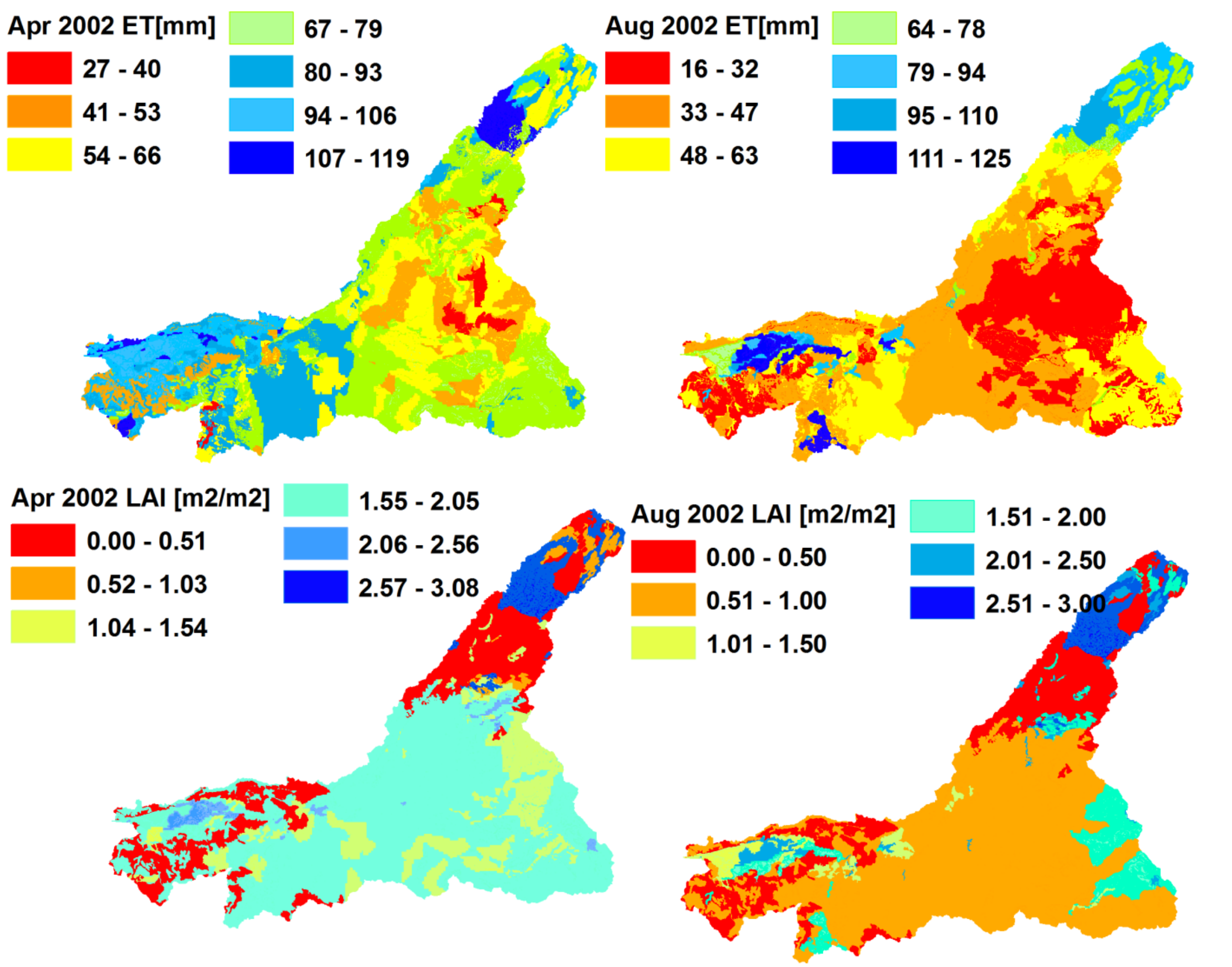

Figure 11 SWAT-T simulated monthly ET (upper row) and LAI (lower row) for April (wet) and August (dry) 2002 at HRU level.

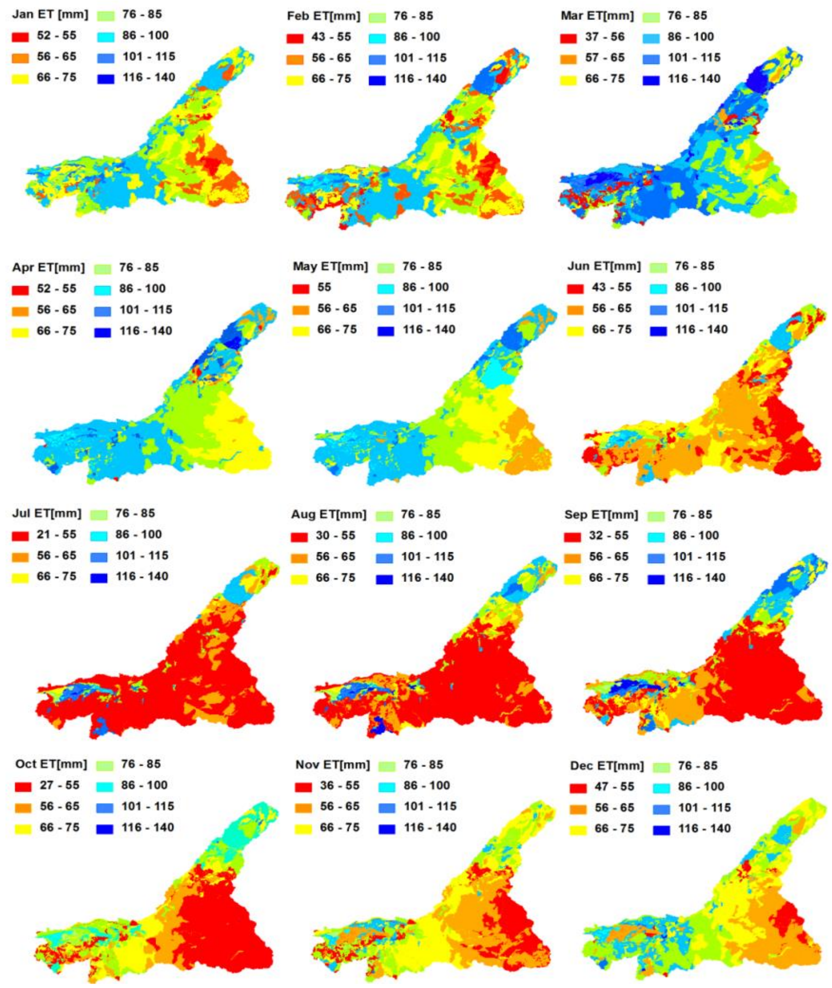

Figure 12 The average seasonal and spatial distribution of ET (2002-2009) in the Mara Basin, as simulated by the SWAT-T model at HRU level.

3.2.4. The performance of the streamflow simulations

Figure 13 presents the comparison of daily SWAT-T simulated streamflow with observation for the calibration and validation periods. Visually, the simulated hydrograph fairly reproduced the observations. The average biases of the SWAT-T simulated daily streamflow compared to observations are 3.5 and 15.5% during the calibration and validation periods, respectively (Table 3). The correlation between the daily observed and simulated streamflows is about 0.72 (0.76) during calibration (validation) period. Additionally, the overall comprehensive assessment using KGE is about 0.71, suggesting the ability of the calibrated SWAT-T model in reproducing observed streamflow responses. However, the model tends to underestimate the baseflow and this is more pronounced during the validation period. This is probably associated with the overestimation of the ET for evergreen forest (6.6%) during the validation, since ET has a known effect on the groundwater flow.

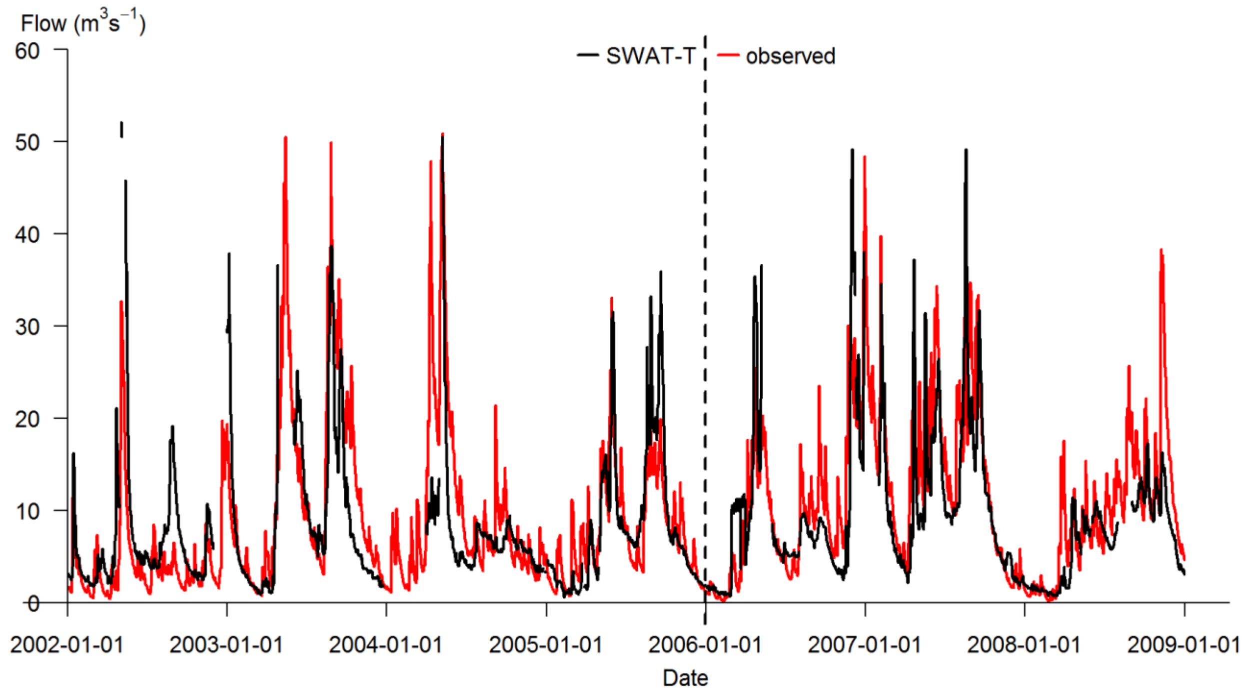

Figure 13 Observed and simulated flows for the Nyangores River at Bomet.

4. Summary and conclusions

We presented an innovative approach to improve the simulation of the annual growth cycle for trees and perennials - and hence improve the simulation of evapotranspiration and streamflow- for tropical conditions in SWAT. The robustness of the changes made to the standard SWAT2012 version 627 have been assessed by comparing the model outputs with remotely sensed 8-day composite Moderate Resolution Imaging Spectroscopy (MODIS) LAI data, as well as with thermal-based evapotranspiration (ET-RS) and observed streamflow data. Towards this, we presented a straightforward but robust soil moisture index (SMI), a quotient of rainfall (P) and reference evapotranspiration (PET), to trigger a new growing season within a defined period. The new growing season starts when the SMI index exceeds or equals a certain user defined threshold.

The structural improvements in the LAI simulation have been demonstrated by comparing uncalibrated simulation of LAI using standard SWAT model and SWAT-T model. The results indicated that the modified module structure for the vegetation growth exhibits temporal progression patterns that are consistent with the seasonal rainfall pattern in the Mara Basin. Further, we noted better consistency in the SWAT-T model simulated potential transpiration for perennial and trees, suggesting the usefulness of the vegetation growth module modification in reducing the model structural uncertainty. Our calibrated SWAT-T model results also show that the calibrated SWAT-T simulated LAI corresponds well with the MODIS LAI for various land cover classes with correlation of up to 0.94, indicating the realistic representation of the start of the new growing season using the SMI after a pre-defined period. The improvement in the vegetation growth cycle in SWAT is also supported with a good agreement of simulated ET with

ET-RS, particularly for the grassland. Additionally, the daily flow simulated with the SWAT-T mimics well the observed flows for the Nyangores River. Therefore, the SWAT-T developed in this study can a robust tool for simulating the vegetation growth dynamics consistently in hydrologic model applications including land use and climate change impact studies.

5. Acknowledgments

We would like to thank Tirthankar Roy, the University of Arizona, for providing bias-corrected satellite rainfall products. We also would like to thank the Water Resource Management Authority (WRMA) of Kenya for provision of streamflow data. The technical help on FORTRAN coding from Befekadu Woldegeorgis, Vrije Universiteit Brussel, is very much appreciated.

6. Data Availability

The modified SWAT model for Tropics is available upon request from the first author.

7. References

Alemayehu, T., van Griensven, A. and Bauwens, W.: Evaluating CFSR and WATCH Data as Input to SWAT for the Estimation of the Potential Evapotranspiration in a Data-Scarce Eastern-African Catchment, J. Hydrol. Eng., 21(3), 5015028, doi:10.1061/(ASCE)HE.1943-5584.0001305, 2015.

Alemayehu, T., Griensven, A. van, Senay, G. B. and Bauwens, W.: Evapotranspiration Mapping in a Heterogeneous Landscape Using Remote Sensing and Global Weather Datasets: Application to the Mara Basin, East Africa, Remote Sens., 9(4), 390, doi:10.3390/rs9040390, 2017.

Andersen, J., Dybkjaer, G., Jensen, K. H., Refsgaard, J. C. and Rasmussen, K.: Use of remotely sensed precipitation and leaf area index in a distributed hydrological model, J. Hydrol., 264(1–4), 34–50, doi:10.1016/S0022-1694(02)00046-X, 2002.

Arnold, J. G., Srinivasan, R., Muttiah, R. S. and Williams, J. R.: Large area hydrologic modeling and assessment part I: model development, J. Am. Water Resour. Assoc., 34(1), 73–89, doi:10.1111/j.1752-1688.1998.tb05961.x, 1998.

Arnold, J. G., D. N. Moriasi, P. W. Gassman, K. C. Abbaspour, M. J. White, R. Srinivasan, C. Santhi, R. D. Harmel, A. van Griensven, M. W. Van Liew, N. Kannan and M. K. Jha: SWAT: Model Use, Calibration, and Validation, Trans. ASABE, 55(4), 1491–1508, doi:10.13031/2013.42256, 2012.

Bobée, C., Ottlé, C., Maignan, F., De Noblet-Ducoudré, N., Maugis, P., Lézine, A. M. and Ndiaye, M.: Analysis of vegetation seasonality in Sahelian environments using MODIS LAI, in association with land cover and rainfall, J. Arid Environ., 84, 38–50, doi:10.1016/j.jaridenv.2012.03.005, 2012.

Bressiani, D. de A., Gassman, P. W., Fernandes, J. G., Garbossa, L. H. P., Srinivasan, R., Bonumá, N. B. and Mendiondo, E. M.: A review of soil and water assessment tool (SWAT) applications in Brazil: Challenges and prospects, Int. J. Agric. Biol. Eng., 8(3), 1–27, doi:10.3965/j.ijabe.20150803.1765, 2015.

Dessu, S. B. and Melesse, A. M.: Modelling the rainfall-runoff process of the Mara River basin using the Soil and Water Assessment Tool, Hydrol. Process., 26(26), 4038–4049, doi:10.1002/hyp.9205, 2012.

DeVries, B., Verbesselt, J., Kooistra, L. and Herold, M.: Robust monitoring of small-scale forest disturbances in a tropical montane forest using Landsat time series, Remote Sens. Environ., 161, 107–121, doi:10.1016/j.rse.2015.02.012, 2015.

Easton, Z. M., Fuka, D. R., White, E. D., Collick, a. S., Biruk Ashagre, B., McCartney, M., Awulachew, S. B., Ahmed, a. a. and Steenhuis, T. S.: A multi basin SWAT model analysis of runoff and sedimentation in the Blue Nile, Ethiopia, Hydrol. Earth Syst. Sci., 14(10), 1827–1841, doi:10.5194/hess-14-1827-2010, 2010.

FAO: Africover Regional Land Cover Database, http://www.africover.org, 2002.

FAO/IIASA/ISRIC/ISSCAS/JRC: Harmonized World Soil Database (version 1.1). FAO,Rome, Italy and IIASA, Laxenburg, Austria., 2009.

FAO, I.-C.: Harmonized World Soil Database (version 1.0), FAO, Rome, Italy a nd IIASA, Laxenburg, Austr., 2008.

Gassman, P. W., Sadeghi, A. M. and Srinivasan, R.: Applications of the SWAT Model Special Section: Overview and Insights, J. Environ. Qual., 43(1), 1, doi:10.2134/jeq2013.11.0466, 2014.

Gebremicael, T. G., Mohamed, Y. A., Betrie, G. D., van der Zaag, P. and Teferi, E.: Trend analysis of runoff and sediment fluxes in the Upper Blue Nile basin: A combined analysis of statistical tests, physically-based models and landuse maps, J. Hydrol., 482, 57–68, doi:10.1016/j.jhydrol.2012.12.023, 2013.

Githui, F., Mutua, F. and Bauwens, W.: Estimating the impacts of land-cover change on runoff using the soil and water assessment tool (SWAT): case study of Nzoia catchment, Kenya / Estimation des impacts du changement d’occupation du sol sur l’écoulement à l’aide de SWAT: étude du cas du bassi, Hydrol. Sci. J., 54(5), 899–908, doi:10.1623/hysj.54.5.899, 2009.

van Griensven, a., Ndomba, P., Yalew, S. and Kilonzo, F.: Critical review of SWAT applications in the upper Nile basin countries, Hydrol. Earth Syst. Sci., 16(9), 3371–3381, doi:10.5194/hess-16-3371-2012, 2012.

Gupta, H. V, Kling, H., Yilmaz, K. K. and Martinez, G. F.: Decomposition of the mean squared error and NSE performance criteria: Implications for improving hydrological modelling, J. Hydrol., 377(1–2), 80–91, doi:10.1016/j.jhydrol.2009.08.003, 2009.

Jolly, W. M. . and Running, S. W.: Effects of precipitation and soil water potential on drought deciduous phenology in the Kalahari, Glob. Chang. Biol., 10(3), 303–308, doi:10.1046/j.1529-8817.2003.00701.x, 2004.

Kilonzo, F.: Assessing the Impacts of Environmental Changes on the Water Resources of the Upper Mara, Lake Victoria Basin. PhD Thesis,Vrije Universiteit Brussel (VUB)., 2014.

Kraus, T.: Ground-based Validation of the MODIS Leaf Area Index Product for East African Rain Forest Ecosystems., 2008.

Kraus, T., Schmidt, M., Dech, S. W. and Samimi, C.: The potential of optical high resolution data for the assessment of leaf area index in East African rainforest ecosystems, Int. J. Remote Sens., 30(19), 5039–5059, doi:Doi 10.1080/01431160903022878, 2009.

Krysanova, V. and White, M.: Advances in water resources assessment with SWAT—an overview, Hydrol. Sci. J., (August), 1–13, doi:10.1080/02626667.2015.1029482, 2015.

Lotsch, A.: Coupled vegetation-precipitation variability observed from satellite and climate records, Geophys. Res. Lett., 30(14), 1774, doi:10.1029/2003GL017506, 2003.

LPDAAC: Land Processes Distributed Active Archive Center (LPDAAC) of NASA, [online] Available from: url: https://lpdaac.usgs.gov/data_access/data_pool (Accessed 5 December 2014), 2014.

Mango, L. M., Melesse, a. M., McClain, M. E., Gann, D. and Setegn, S. G.: Land use and climate change impacts on the hydrology of the upper Mara River Basin, Kenya: results of a modeling study to support better resource management, Hydrol. Earth Syst. Sci., 15(7), 2245–2258, doi:10.5194/hess-15-2245-2011, 2011.

Maranda, B. and Anctil, F.: SWAT Performance as Influenced by Potential Evapotranspiration Formulations in a Canadian Watershed, Trans. ASABE, 58(6), 1585–1600, doi:10.13031/trans.58.11290, 2015.

Mengistu, D. T. and Sorteberg, a.: Sensitivity of SWAT simulated streamflow to climatic changes within the Eastern Nile River basin, Hydrol. Earth Syst. Sci., 16(2), 391–407, doi:10.5194/hess-16-391-2012, 2012.

Monteith, J. L.: Evaporation and the environment, The state and movement of water in living organisms, in XIXth symposium, Cambridge University Press, Swansea., 1965.

Mwangi, H. M., Julich, S., Patil, S. D., McDonald, M. a. and Feger, K.-H.: Modelling the impact of agroforestry on hydrology of Mara River Basin in East Africa, Hydrol. Process., n/a-n/a, doi:10.1002/hyp.10852, 2016.

Myneni, R. ., Hoffman, S., Knyazikhin, Y., Privette, J. ., Glassy, J., Tian, Y., Wang, Y., Song, X., Zhang, Y., Smith, G. ., Lotsch, A., Friedl, M., Morisette, J. ., Votava, P., Nemani, R. . and Running, S. .: Global products of vegetation leaf area and fraction absorbed PAR from year one of MODIS data, Remote Sens. Environ., 83(1–2), 214–231, doi:10.1016/S0034-4257(02)00074-3, 2002.

Myneni, R. B., Yang, W., Nemani, R. R., Huete, A. R., Dickinson, R. E., Knyazikhin, Y., Didan, K., Fu, R., Negron Juarez, R. I., Saatchi, S. S., Hashimoto, H., Ichii, K., Shabanov, N. V, Tan, B., Ratana, P., Privette, J. L., Morisette, J. T., Vermote, E. F., Roy, D. P., Wolfe, R. E., Friedl, M. a, Running, S. W., Votava, P., El-Saleous, N., Devadiga, S., Su, Y. and Salomonson, V. V: Large seasonal swings in leaf area of Amazon rainforests, Proc. Natl. Acad. Sci., 104(12), 4820–4823, doi:10.1073/pnas.0611338104, 2007.

NASA: United States Geological Survey Earth Explorer. Available online: http://earthexplorer.usgs.gov/ (accessed on 9 Sept 2015)., [online] Available from: http://earthexplorer.usgs.gov/, 2014.

Neitsch, S. L., Arnold, J. G., Kiniry, J. R. and Williams, J. R.: Soil & Water Assessment Tool Theoretical Documentation Version 2009.Texas Water Resources Institute Technical Report No. 406 Texas A&M University System College Station, TX,pp. 647., 2011.

Pfeifer, M., Gonsamo, A., Disney, M., Pellikka, P. and Marchant, R.: Leaf area index for biomes of the Eastern Arc Mountains: Landsat and SPOT observations along precipitation and altitude gradients, Remote Sens. Environ., 118(2012), 103–115, doi:10.1016/j.rse.2011.11.009, 2012.

Pfeifer, M., Lefebvre, V., Gonsamo, A., Pellikka, P. K. E., Marchant, R., Denu, D. and Platts, P. J.: Validating and linking the GIMMS leaf area index (LAI3g) with environmental controls in tropical Africa, Remote Sens., 6(3), 1973–1990, doi:10.3390/rs6031973, 2014.

Ritchie, J. T.: Model for predicting evaporation from a row crop with incomplete cover, Water Resour. Res., 8(5), 1204–1213, doi:10.1029/WR008i005p01204, 1972.

Rodell, M., Houser, P. R., Jambor, U., Gottschalck, J., Mitchell, K., Meng, C.-J., Arsenault, K., Cosgrove, B., Radakovich, J., Bosilovich, M., Entin, J. K., Walker, J. P., Lohmann, D. and Toll, D.: The Global Land Data Assimilation System, Bull. Am. Meteorol. Soc., 85(March), 381–394, doi:10.1175/BAMS-85-3-381, 2004.

Roy, T., Serrat-Capdevila, A., Gupta, H. and Valdes, J.: A platform for probabilistic Multimodel and Multiproduct Streamflow Forecasting, Water Resour. Res., (3), 1–24, doi:10.1002/2016WR019752, 2017.

Sacks, W. J., Deryng, D., Foley, J. A. and Ramankutty, N.: Crop planting dates: an analysis of global patterns, Glob. Ecol. Biogeogr., 19, no-no, doi:10.1111/j.1466-8238.2010.00551.x, 2010.

Senay, G. B., Bohms, S., Singh, R. K., Gowda, P. H., Velpuri, N. M., Alemu, H. and Verdin, J. P.: Operational Evapotranspiration Mapping Using Remote Sensing and Weather Datasets: A New Parameterization for the SSEB Approach, JAWRA J. Am. Water Resour. Assoc., 49(3), 577–591, doi:10.1111/jawr.12057, 2013.

Setegn, S. G., Srinivasan, R., Melesse, A. M. and Dargahi, B.: SWAT model application and prediction uncertainty analysis in the Lake Tana Basin, Ethiopia, Hydrol. Process., 24(3), 357–367, doi:10.1002/hyp.7457, 2009.

Setegn, S. G., Rayner, D., Melesse, A. M., Dargahi, B. and Srinivasan, R.: Impact of climate change on the hydroclimatology of Lake Tana Basin, Ethiopia, Water Resour. Res., 47(4), n/a-n/a, doi:10.1029/2010WR009248, 2011.

Shen, C., Niu, J. and Phanikumar, M. S.: Evaluating controls on coupled hydrologic and vegetation dynamics in a humid continental climate watershed using a subsurface-land surface processes model, Water Resour. Res., 49(5), 2552–2572, doi:10.1002/wrcr.20189, 2013.

Strauch, M.: SWAT plant growth modification for improved modeling of tropical vegetation SWAT is increasingly used in the tropics …, 2013.

Strauch, M. and Volk, M.: SWAT plant growth modification for improved modeling of perennial vegetation in the tropics, Ecol. Modell., 269, 98–112, doi:10.1016/j.ecolmodel.2013.08.013, 2013.

Teklesadik, A. D., Alemayehu, T., van Griensven, A., Kumar, R., Liersch, S., Eisner, S., Tecklenburg, J., Ewunte, S. and Wang, X.: Inter-model comparison of hydrological impacts of climate change on the Upper Blue Nile basin using ensemble of hydrological models and global climate models, Clim. Change, doi:10.1007/s10584-017-1913-4, 2017.

Trabucco, A. and Zomer, R. J.: Global Aridity Index (Global-Aridity) and Global Potential Evapo-Transpiration (Global-PET) Geospatial Database. CGIAR Consortium for Spatial Information. Published online, available from the CGIAR-CSI GeoPortal, 2009.

USDA SCS: Section 4 Hydrology, National Engineering Handbook. Washington., 1972.

Verbesselt, J., Hyndman, R., Newnham, G. and Culvenor, D.: Detecting trend and seasonal changes in satellite image time series, Remote Sens. Environ., 114(1), 106–115, doi:10.1016/j.rse.2009.08.014, 2010.

Verbesselt, J., Zeileis, A. and Herold, M.: Near real-time disturbance detection using satellite image time series, Remote Sens. Environ., 123(2012), 98–108, doi:10.1016/j.rse.2012.02.022, 2012.

Wagner, P. D., Kumar, S., Fiener, P. and Schneider, K.: Hydrological Modeling with SWAT in a Monsoon -Driven environment: Experience from the Western Ghats, India, Trans. ASABE, 54(5), 1783–1790, 2011.

Wang, X., Melesse, A. M. and Yang, W.: Influences of Potential Evapotranspiration Estimation Methods on SWAT's Hydrologic Simulation in a Northwestern Minnesota Watershed, Trans. ASABE, 49(6), 1755–1771, doi:10.13031/2013.22297, 2006.

Yang, Q. and Zhang, X.: Improving SWAT for simulating water and carbon fluxes of forest ecosystems, Sci. Total Environ., 569–570, 1478–1488, doi:10.1016/j.scitotenv.2016.06.238, 2016.

Yu, X., Lamačová, A., Duffy, C., Krám, P. and Hruška, J.: Hydrological model uncertainty due to spatial evapotranspiration estimation methods, Comput. Geosci., 90(2016), 90–101, doi:10.1016/j.cageo.2015.05.006, 2016.

Zhang, K., Kimball, J. S., Nemani, R. R. and Running, S. W.: A continuous satellite-derived global record of land surface evapotranspiration from 1983 to 2006, Water Resour. Res., 46(9), 1–21, doi:10.1029/2009WR008800, 2010.

Zhang, X.: Monitoring the response of vegetation phenology to precipitation in Africa by coupling MODIS and TRMM instruments, J. Geophys. Res., 110(D12), D12103, doi:10.1029/2004JD005263, 2005.

Zhang, X., Friedl, M. A. and Schaaf, C. B.: Global vegetation phenology from Moderate Resolution Imaging Spectroradiometer (MODIS): Evaluation of global patterns and comparison with in situ measurements, J. Geophys. Res. Biogeosciences, 111(4), 1–14, doi:10.1029/2006JG000217, 2006.

Zhang, Y., Chiew, F. H. S., Zhang, L. and Li, H.: Use of Remotely Sensed Actual Evapotranspiration to Improve Rainfall–Runoff Modeling in Southeast Australia, J. Hydrometeorol., 10(4), 969–980, doi:10.1175/2009JHM1061.1, 2009.